patient B (Table 1). Patient C was probably not a SaV re-infection case, because SaV shedding can last for 1-4 weeks after gastroenteritis symptoms subside, as reported previously [11]. Indeed, the patient recovered from diarrhea but 18 days later had different symptoms (i.e., vomiting) (Table 1), and the two stool samples from patient C contained the same genotype of SaV with 99.0 % (606/ 612) nucleotide sequence identity within the partial capsid region (data not shown). Furthermore, the SaV RNA load from a stool specimen at the second visit was 4 $\log_{10}$ lower than that at the first visit, and high levels of GII NoV were detected at the second visit, coincident with the vomiting observed (Table 1). Thus, we conclude that the vomiting of patient C at the second visit was likely due to NoV infection.

Nakata et al. reported a significant rise in antibody levels after SaV infection, and serum anti-SaV antibody levels may correlate with resistance to SaV gastroenteritis [15]. However, our results suggest that protective immunity may be at least genogroup-specific for SaV or that protective immunity does not last for a long time. A follow-up survey can provide additional information to answer this question, because serum samples were not collected in our study.

The 139 SaV strains detected from 2002 to 2011 were classified into four genogroups and 11 genotypes: GI.1 (n=26), GI.2 (n=3), GI.3 (n=2), GI.6 (n=4), GII.1 (n=12), GII.2 (n=4), GII.3 (n=29), GII.4 (n=1), GII.7 (n=1), GIV (n=51) and GV (n=6) (Table 2). GIV SaVs were predominant in 2007, as reported previously [8], but they were not detected in 2008-2011. Instead, GII.3 SaVs became predominant in 2008 and then gradually decreased in 2009 and 2010 (Table 2). The SaV capsid-encoding region is highly diverse among different genogroups/genotypes at both the nucleic acid and amino acid sequence level [3, 7, 18, 19], and SaV strains of different genogroups and genotypes have distinct antigenicities [4, 6, 7, 12, 17]. Such genogroup/genotype shifts of SaVs in the population in the same geographic area may be due to herd immunity, although further study is required to assess this.

In conclusion, we found SaV re-infection gastroenteritis case(s) for the first time. Our data indicate that people can be sequentially infected with SaVs of different genogroups during their life and that they may suffer from gastroenteritis after each infection, as was clearly evident for patient A. We also found a genetic shift in SaV among the gastroenteritis outpatients in the same restricted geographical location. Global SaV surveillance and seroprevalence studies are warranted to investigate whether such re-infections and genetic shifts occur in other geographic areas and whether SaV protective immunity is genogroup/genotype-specific.

Acknowledgments This work was supported in part by a grant for Research on Emerging and Re-emerging Infectious Diseases from the Ministry of Health, Labour, and Welfare of Japan.

References

1. Cheng WX, Ye XH, Yang XM, Li YN, Jin M, Jin Y, Duan ZJ (2010) Epidemiological study of human calicivirus infection in children with gastroenteritis in Lanzhou from 2001 to 2007. Arch Virol 155:553–555
2. Chiba S, Nakata S, Numata-Kinoshita K, Honma S (2000) Sapporo virus: history and recent findings. J Infect Dis 181(Suppl 2): S303–S308
3. Farkas T, Zhong WM, Jing Y, Huang PW, Espinosa SM, Martinez N, Morrow AL, Ruiz-Palacios GM, Pickering LK, Jiang X (2004) Genetic diversity among sapoviruses. Arch Virol 149: 1309–1323
4. Farkas T, Deng X, Ruiz-Palacios G, Morrow A, Jiang X (2006) Development of an enzyme immunoassay for detection of sapovirus-specific antibodies and its application in a study of seroprevalence in children. J Clin Microbiol 44:3674–3679
5. Gallimore CI, Iturriza-Gomara M, Lewis D, Cubitt D, Cotterill H, Gray JJ (2006) Characterization of sapoviruses collected in the United Kingdom from 1989 to 2004. J Med Virol 78:673–682
6. Hansman GS, Natori K, Oka T, Ogawa S, Tanaka K, Nagata N, Ushijima H, Takeda N, Katayama K (2005) Cross-reactivity among sapovirus recombinant capsid proteins. Arch Virol 150: 21–36
7. Hansman GS, Oka T, Sakon N, Takeda N (2007) Antigenic diversity of human sapoviruses. Emerg Infect Dis 13:1519–1525
8. Harada S, Okada M, Yahiro S, Nishimura K, Matsuo S, Miyasaka J, Nakashima R, Shimada Y, Ueno T, Ikezawa S, Shinozaki K, Katayama K, Wakita T, Takeda N, Oka T (2009) Surveillance of pathogens in outpatients with gastroenteritis and characterization of sapovirus strains between 2002 and 2007 in Kumamoto Prefecture, Japan. J Med Virol 81:1117–1127
9. Iizuka S, Oka T, Tabara K, Omura T, Katayama K, Takeda N, Noda M (2010) Detection of sapoviruses and noroviruses in an outbreak of gastroenteritis linked genetically to shellfish. J Med Virol 82:1247–1254
10. Iturriza-Gomara M, Elliot AJ, Dockery C, Fleming DM, Gray JJ (2009) Structured surveillance of infectious intestinal disease in pre-school children in the community: 'The Nappy Study'. Epidemiol Infect 137:922–931
11. Iwakiri A, Ganmyo H, Yamamoto S, Otao K, Mikasa M, Kizoe S, Katayama K, Wakita T, Takeda N, Oka T (2009) Quantitative analysis of fecal sapovirus shedding: identification of nucleotide substitutions in the capsid protein during prolonged excretion. Arch Virol 154:689–693
12. Jiang X, Cubitt WD, Berke T, Zhong W, Dai X, Nakata S, Pickering LK, Matson DO (1997) Sapporo-like human caliciviruses are genetically and antigenically diverse. Arch Virol 142: 1813–1827
13. Johansson PJ, Bergentoft K, Larsson PA, Magnusson G, Widell A, Thorhagen M, Hedlund KO (2005) A nosocomial sapovirus-associated outbreak of gastroenteritis in adults. Scand J Infect Dis 37:200–204
14. Mayo MA (2002) A summary of taxonomic changes recently approved by ICTV. Arch Virol 147:1655–1663
15. Nakata S, Chiba S, Terashima H, Yokoyama T, Nakao T (1985) Humoral immunity in infants with gastroenteritis caused by human calicivirus. J Infect Dis 152:274–279
16. Oka T, Katayama K, Hansman GS, Kageyama T, Ogawa S, Wu FT, White PA, Takeda N (2006) Detection of human sapovirus by

real-time reverse transcription-polymerase chain reaction. J Med Virol 78:1347–1353
17. Oka T, Miyashita K, Katayama K, Wakita T, Takeda N (2009) Distinct genotype and antigenicity among genogroup II sapoviruses. Microbiol Immunol 53:417–420
18. Oka T, Mori K, Iritani N, Harada S, Ueki Y, Iizuka S, Mise K, Murakami K, Wakita T, Katayama K (2012) Human sapovirus classification based on complete capsid nucleotide sequences. Arch Virol 157:349–352
19. Okada M, Yamashita Y, Oseto M, Ogawa T, Kaiho I, Shinozaki K (2006) Genetic variability in the sapovirus capsid protein. Virus Genes 33:157–161
20. Okada M, Yamashita Y, Oseto M, Shinozaki K (2006) The detection of human sapoviruses with universal and genogroup-specific primers. Arch Virol 151:2503–2509
21. Pang XL, Lee BE, Tyrrell GJ, Preiksaitis JK (2009) Epidemiology and genotype analysis of sapovirus associated with gastroenteritis outbreaks in Alberta, Canada: 2004–2007. J Infect Dis 199:547–551
22. Phan TG, Okame M, Nguyen TA, Maneekarn N, Nishio O, Okitsu S, Ushijima H (2004) Human astrovirus, norovirus (GI, GII), and sapovirus infections in Pakistani children with diarrhea. J Med Virol 73:256–261
23. Sdiri-Loulizi K, Hassine M, Gharbi-Khelifi H, Aouni Z, Chouchane S, Sakly N, Neji-Guediche M, Pothier P, Ambert-Balay K, Aouni M (2011) Molecular detection of genogroup I sapovirus in Tunisian children suffering from acute gastroenteritis. Virus Genes 43:6–12
24. Svraka S, Vennema H, van der Veer B, Hedlund KO, Thorhagen M, Siebenga J, Duizer E, Koopmans M (2010) Epidemiology and genotype analysis of emerging sapovirus-associated infections across Europe. J Clin Microbiol 48:2191–2198
25. Yoshida T, Kasuo S, Azegami Y, Uchiyama Y, Satsumabayashi K, Shiraishi T, Katayama K, Wakita T, Takeda N, Oka T (2009) Characterization of sapoviruses detected in gastroenteritis outbreaks and identification of asymptomatic adults with high viral load. J Clin Virol 45:67–71

Exp. Anim. 61(1), 35–40, 2012

—Original—

Evaluation of Four Antiseptics Using a Novel Murine Norovirus

Takashi MATSUHIRA[1)], Chizuko KAJI[1)], Shoichi MURAKAMI[1)], Kazunori MAEBASHI[1)], Tomoichiro OKA[2)], Naokazu TAKEDA[3)], and Kazuhiko KATAYAMA[2)]

[1)]Pharmaceutical Research Center, Meiji Seika Pharma Co., Ltd., 760 Morooka-cho, Kohoku-ku, Yokohama 222-8567, [2)]Department of Virology II, National Institute of Infectious Diseases, 4–7–1 Gakuen, Musashi-murayama, Tokyo 208-0011, Japan, and [3)]Section of Viral Infections, Thailand-Japan Research Collaboration Center on Emerging and Re-Emerging Infections (RCC-ERI), 6th Fl., Building 10, Department of Medical Sciences, Ministry of Publlic Health, Tiwanon Rd., Muang, Nonthaburi 11000, Thailand

Abstract: We isolated a novel murine norovirus (MNV), MT30-2 strain, from feces of conventional mice in Japan to evaluate the virucidal activity of four antiseptics. The MNV MT30-2 strain was inactivated by as little as 0.2% (w/v) povidone-iodine (PVP-I) and 0.1% (w/v) sodium hypochlorite (NaOCl) treatment as determined by a novel plaque assay. Importantly, PVP-I reduced the MNV titer by 4 $\log_{10}$ within 15 s of exposure. The other two antiseptics, benzethonium chloride (BEC) and chlorhexidine gluconate (CHG), did not reduce the MNV titer even when treatment lasted for 60 s. When the virus titer was reduced by PVP-I or NaOCl treatment, the amount of MNV RNA was not reduced, indicating that the presence of viral RNA was not related to the virucidal activity of the antiseptics. PVP-I and NaOCl will be useful in controlling the spread of MNV, which is a common problem in mice colonies. In this study, we isolated a novel MNV and newly revealed that two antiseptics (PVP-I and NaOCl) were able to inactivate MNV at low concentrations and in a short contact time.

Key words: antiseptics, murine norovirus, plaque assay, quantitative RT-PCR

Introduction

Noroviruses belong to a group of single-stranded RNA, nonenveloped viruses in the Caliciviridae family that are widely transmitted among humans or animals. At present, five major genogroups (GI-GV) of noroviruses have been designated, with GI, GII, and GIV infecting humans, GIII infecting bovines, and GV infecting murines [17]. Murine norovirus (MNV), prototype MNV-1, was first identified in 2003 in immunocompromised mice lacking recombination-activating gene 2 (RAG2), signal transducer, and activator of transcription 1 (STAT1) (RAG2/STAT1$^{-/-}$) [9]. Human norovirus (HuNoV) cannot grow in cell culture [5]. On the other hand, MNV is the only norovirus capable of replicating in both cell culture and small animals [17, 18]. Infection of MNV in a normal mouse shows no visible signs, but MNV can induce a clinical disease with a high mortality in congenitally immunodeficient mice [13]. The major infection route of MNV is a fecal-oral route, and shedding of MNV continues for at least eight weeks post infection [6–8]. Accordingly, MNV is one of the most

(Received 27 April 2011 / Accepted 25 July 2011)

Address corresponding: T. Matsuhira, Pharmaceutical Research Center, Meiji Seika Pharma Co., Ltd., 760 Morooka-cho, Kohoku-ku, Yokohama 222-8567, Japan

transmittable and prevalent pathogens in laboratory mice today [6, 8, 12], making the prevention of the spread of MNV an important issue.

In a previous study using the MNV CW1 strain [18], the antiseptic effect of ethanol (EtOH) against MNV was examined [1], and 60% (v/v) EtOH was shown to reduce the MNV infectious titer by 4 $\log_{10}$ within 30 s of exposure; however, 30% (v/v) EtOH did not reduce the titer. Moreover, 1% (w/v) povidone-iodine (PVP-I) and 0.26% (w/v) sodium hypochlorite (NaOCl) have been shown to inactivate the MNV CW1 strain, although the efficacies of these antiseptics against other MNV strains are unknown.

In this study, to clarify the virucidal activity of antiseptics against another MNV strain, we isolated a novel MNV, strain MT30-2, from conventional mice in Japan. Using the MT30-2 strain, the virucidal activity of PVP-I was examined. PVP-I has been used as an external treatment for humans and has a broad spectrum of virucidal activity against enveloped and nonenveloped DNA and RNA viruses [10]. We compared the virucidal activity of PVP-I with those of NaOCl, benzethonium chloride (BEC), and chlorhexidine gluconate (CHG) using plaque assays. Furthermore, we quantified MNV MT30-2 RNA copies by quantitative reverse transcription polymerase chain reaction (RT-PCR) and compared the results with virus titers determined in the plaque assay.

Materials and Methods

Mice

Six-week-old male conventional ICR mice were purchased from a conventional Japanese mouse breeder (Chiba, Japan). The mice were kept in a temperature-and light-controlled environment with standard food and water given *ad libitum*. All experiments were approved by the Animal Care and Use Committee of Meiji Seika Pharma Pharmaceutical Research Center.

Cells and virus infection

RAW264.7 cells, a mouse macrophage cell line, were purchased from DS-Pharma (Osaka, Japan) and cultured in high-glucose Dulbecco's modified Eagle medium + GlutaMAX™-I (DMEM; Invitrogen, Carlsbad, CA, USA) supplemented with 25 mM HEPES and 10% fetal bovine serum (FBS) at 37°C in 5% CO_2. MNV was inoculated onto a monolayer of RAW264.7 cells, and cultured in DMEM supplemented with 25 mM HEPES and 2% FBS (DMEM-2% FBS) at 37°C in 5% CO_2. Three to 5 days later, the cultured medium was centrifuged at 15,000 *g* for 5 min at 4°C, and the supernatant was used as the virus stock.

Isolation of MNV

Two stool samples per mouse were collected, homogenized in PBS, and then centrifuged at 15,000 *g* for 15 min at room temperature. The supernatant was passed through a 0.22-μm-pore-size filter, diluted in DMEM-2% FBS, and used to inoculate RAW264.7 cells. Four days later, the culture medium and RAW264.7 cells were frozen at –80°C. After thawing, the culture medium and cells were centrifuged at 8,000 *g* for 5 min at 4°C, and the supernatant was used for further passage. A total of nine passages followed by two successive plaque purifications were performed. Plaque assays were performed as previously described [18] with RAW264.7 cells.

MNV inactivation experiment

Different antiseptics were used to inactivate the MNV. PVP-I (ISODINE solution 10%) was obtained from Meiji Seika Pharma (Tokyo, Japan). NaOCl (Purelox-S) was purchased from Oyalox (Tokyo, Japan). BEC (Hyamine solution 10%) was purchased from Daiichi Sankyo (Tokyo, Japan). CHG (Hibitane gluconate 20%) was purchased from Dainippon Sumitomo Pharma (Osaka, Japan). Inactivation was induced by adding 100 μl of the diluted antiseptic [0.4 or 2% (w/v) PVP-I, 0.2 or 0.4% (w/v) NaOCl, 0.2% (w/v) BEC, 1% (w/v) CHG] to 100 μl of virus stock solution. The final volume of 200 μl reaction mixture was incubated for 15, 30, 45 or 60 s at room temperature prior to neutralization. Neutralization control samples were used as 0-s incubation samples. To stop the effect of PVP-I, 2 μl of 1 M sodium thiosulfate was added to the reaction mixture. To stop the effect of NaOCl, 10 μl of 1 M sodium thiosulfate was added to the reaction mixture, followed by 10 μl of 1 M HEPES (pH 7.4). The neutralized solutions obtained from the above treatment were then 10-fold diluted with DMEM-2% FBS. For the neutralization control, PVP-I and NaOCl were first neutralized with sodium thiosulfate

and diluted with DMEM-2% FBS before being added to the virus stock. To stop the effect of BEC and CHG, the reaction mixtures were 100-fold diluted with DMEM-2% FBS. The neutralization controls for BEC and CHG were prepared by diluting the virus stock with DMEM-2% FBS without adding antiseptics. The virus titer and copy numbers of MNV RNA in the reaction mixture were measured by plaque assays and quantitative RT-PCR, respectively.

RT-PCR

Viral RNA was extracted from the fecal suspension or supernatant using QIAamp Viral RNA Mini Kits (QIAGEN, Valencia, CA, USA) according to the manufacturer's instructions. An RT-PCR primer pair (forward, 5'-TTTGGAACAATGGATGCTGA-3'; reverse, 5'-TAGGGTGGTACAAGGGCAAC-3') was designed against the conserved capsid sequences of MNV-1 (GenBank accession No. AY228235), MNV-2 (DQ23041), MNV-3 (DQ223042), and MNV-4 (DQ223043). RT-PCR was performed as previously described [7].

Quantitative RT-PCR

Viral RNA was prepared from the reaction mixture using QIAamp Viral RNA Mini Kits. A forward primer (5'-CAGATCACATGCTTCCCACAT-3'), reverse primer (5'-CCAGAGACCACAAAAGACTCATCA-3') and probe (5'FAM -CCCATTCAACTCCCTCTTCTTGA-3'TAMRA) were designed against the conserved sequences of MNV. Quantitative RT-PCR was performed using an EZ RT-PCR Kit (Applied Biosystems, Foster City, CA, USA) and ABI Prism 7700 Sequence Detection System (Applied Biosystems). The following RT-PCR parameters were used: 50°C for 2 min, 60°C for 30 min, 95°C for 5 min, and then 50 cycles of denaturation (94°C, 15 s), annealing (60°C, 30 s), and extension (72°C, 30 s). The standard curve was generated with serial dilutions of MNV-1 RNA encoding the capsid region synthesized by an AmpliScribe T7 Transcription Kit (Epicentre, Madison, WI, USA).

Sequence analysis of viral RNA

Viral RNA was purified from MNV-infected RAW cells with a Purelink Viral RNA/DNA Kit (Invitrogen), and cDNA was synthesized using SuperScript III reverse transcriptase (Invitrogen) and an oligo (dT) primer. Genome-specific sequences were amplified with an Expand Long kit (Roche Applied Science, Indianapolis, IN, USA), and PCR products were sequenced directly with a Taq DyeDeoxy Terminator cycle sequencing kit (Applied Biosystems) on an ABI 3730XL DNA analyzer using MNV1-specific primers. When these primers failed, additional sequence-specific primers were designed and used for sequencing. The termini of the MNV genomes were obtained using GeneRacer (Invitrogen), and sequencing was carried out with sequence-specific primers. The nucleotide and protein sequences of ORF1, ORF2, or ORF3 were aligned using BioEdit (http://www.mbio.ncsu.edu/BioEdit/bioedit.html) and employed for subsequent phylogenetic analyses. A phylogenetic tree with 1,000 bootstrap replications was constructed by the neighbor-joining method. The distance of nucleotide substitutions per site was calculated by Kimura's two-parameter method and was visualized using the NJplot software (http://pbil.univ-lyon1.fr/software/njplot.html). Nucleotide and amino acid sequences were analyzed with GENETYX-MAC version 12.2.6 (Genetyx, Tokyo, Japan).

Nucleotide sequence accession number

The MNV nucleotide sequence determined in this study was deposited in DDBJ under the accession number AB601769.

Results

Isolation and genetic characterization of a novel MNV

To identify MNV-infected mice, fecal samples were collected from eight mice, and RT-PCR was performed using a novel set of primers designed from conserved sites on MNV genomes. The MNV gene was detected in all eight samples (Fig. 1A). A plaque became visible after nine passages with RAW264.7 cells (Fig. 1B). After two rounds of plaque purification, MNV was isolated as a single plaque and designated as MNV MT30-2. The complete nucleotide sequence was determined, and homology searches with other MNV strains showed the MNV MT30-2 strain to be genetically similar to MNV CR3/2005/USA [15] (Fig. 2).

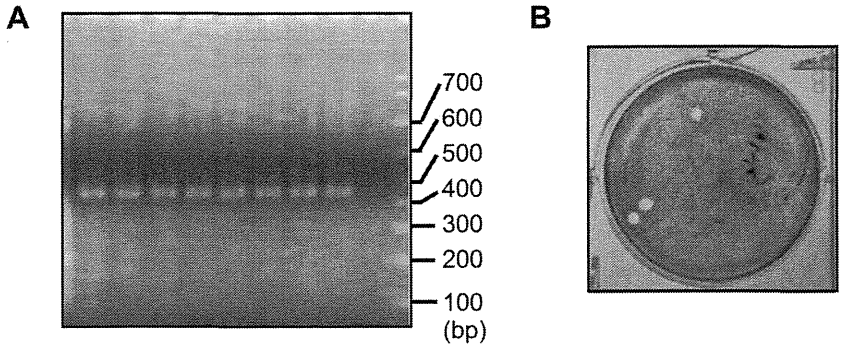

Fig. 1. Detection of MNV gene and MNV plaques. (A) Agarose gel electrophoresis of MNV-specific RT-PCR products (421 bp). (B) Plaques of RAW264.7 cell-adapted MNV.

Table 1. Virucidal effect of PVP-I and NaOCl compared by real-time RT-PCR and plaque assay

Disinfectant	Treatment time (s)	RNA copy no. (log copy no./ml)	Plaque no. (log PFU/ml)
1% (w/v) PVP-I	0	6.69	6.38
	60	6.65	<2.0
0.2% (w/v) NaOCl	0	6.66	6.13
	60	6.30	3.13

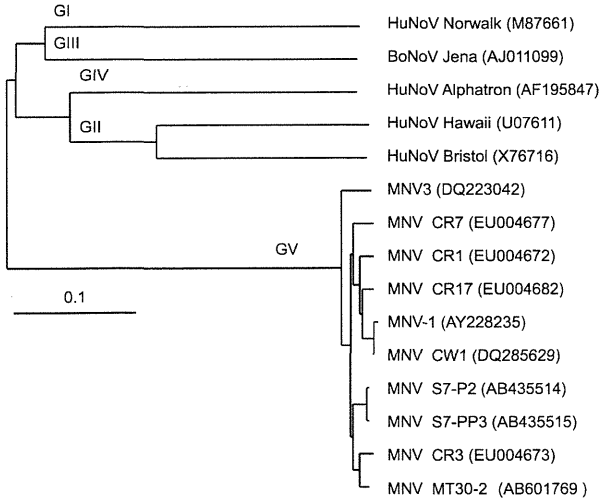

Fig. 2. Phylogenic tree of the Noroviruses. The phylogenic tree was generated using the neighbor-joining method on the basis of an alignment of the entire amino acid sequence of the capsid genes. Numbers in parentheses indicate GenBank accession Nos.

Virucidal activity of antiseptics against MNV

To determine the efficacy of different antiseptics (PVP-I, NaOCl, BEC, and CHG) against the MT30-2 strain, we determined the virus titer using a plaque assay after each antiseptic was added to the virus. Both 0.2 and 1% (w/v) PVP-I reduced the titer by 4 $\log_{10}$ within 15 s (Fig. 3A). Both 0.1 and 0.2% (w/v) NaOCl reduced the titer by 1.6 and 3 $\log_{10}$ in 60 s, respectively (Fig. 3B). In contrast, 0.1% (w/v) BEC and 0.5% (w/v) CHG resulted in only a slight reduction in the titer after 60 s of treatment (Fig. 3C). These results indicated that PVP-I and NaOCl efficiently and rapidly inactivated MNV, whereas both BEC and CHG were ineffective against MNV.

Relationship between plaque assay and quantitative RT-PCR

The effectiveness of antiseptics against a noncultivatable virus is often measured by quantitative RT-PCR. Thus, we quantified MNV MT30-2 RNA copies in samples treated for 60 s with 1% (w/v) PVP-I or 0.2% (w/v) NaOCl and compared the values with the virus titers. We found the number of MNV MT30-2 RNA copies was only slightly reduced when the virus titer was greatly reduced (Table 1), i.e., the quantitative RT-PCR results did not necessarily reflect the plaque assay results.

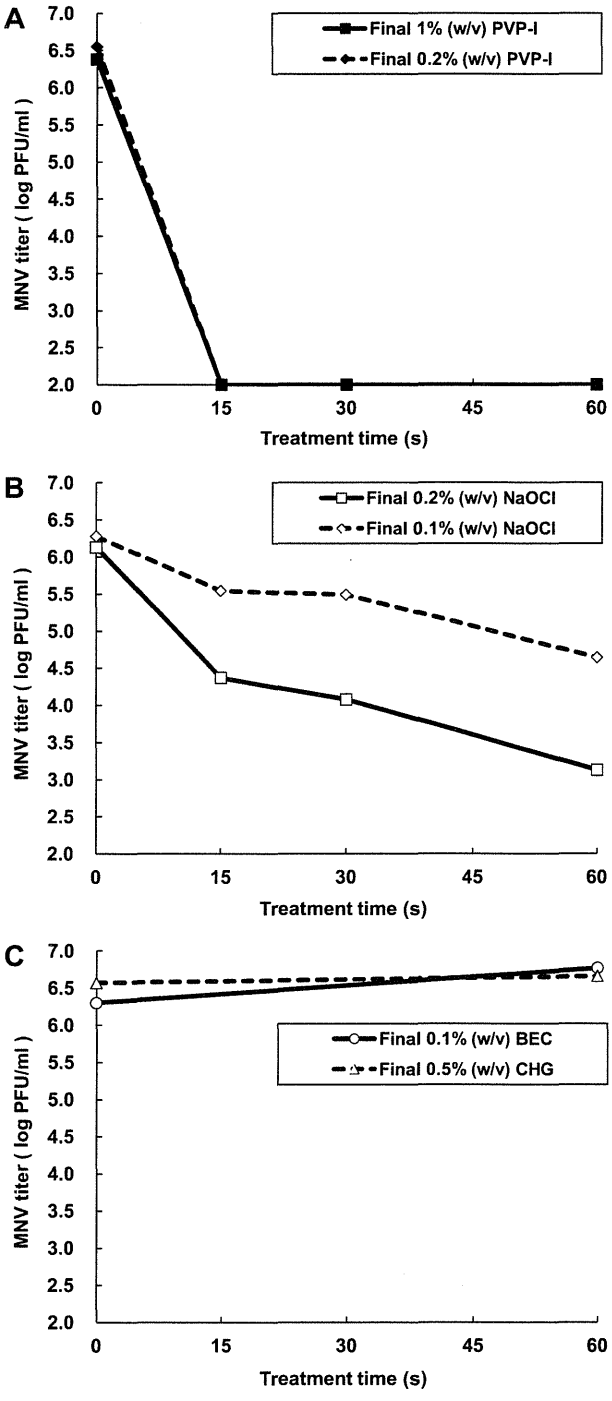

Fig. 3. Virucidal activity of antiseptics against MNV. Each point represents the geometric mean titer (log PFU/ml) of two samples. (A) Effect of PVP-I. Solid squares and solid diamonds indicate the 1% (w/v) and 0.2% (w/v) PVP-I-treated groups, respectively. (B) Effect of NaOCl. Open squares and open diamonds indicate the 0.2% (w/v) and 0.1% (w/v) NaOCl-treated groups, respectively. (C) Effect of BEC and CHG. Open circles and open triangles indicate the 0.1% (w/v) BEC and 0.5% (w/v) CHG-treated groups, respectively.

These results coincided with those in a previous report using MNV CW1 [1].

Discussion

In the present study, we described the isolation of a novel MNV, strain MT30-2. Sequence analysis showed that MT30-2 was genetically similar to MNV CR3/2005/USA (Fig. 2). Using the MT30-2 strain, we showed that two antiseptics (PVP-I and NaOCl) were able to inactivate the virus at low concentrations and in a short contact time (Fig. 3A and 3B). The other two antiseptics, BEC and CHG, which showed virucidal activity against several human viruses [10], appeared to be ineffective against MNV (Fig. 3C). PVP-I and NaOCl also showed strong virucidal activity against MNV CW1 [1], a genetically separated strain from our work (Fig. 2), suggesting that these two antiseptics potentially possess virucidal activity against various MNV strains. EtOH also reduced the MNV infectious titer [1]. However, previous reports demonstrated that EtOH did not show virucidal activity over a short time frame against Feline calicivirus (FCV), another antiseptics-resistant virus that, like MNV, belongs to the *Caliciviridae* family [4, 11]. On the other hand, PVP-I and NaOCl are effective for FCV [3, 4, 11, 16]. Accordingly, PVP-I and NaOCl might be effective against not only other MNV strains but also other related noroviruses including HuNoV.

Since the infectivity of HuNoV is very strong, only a few viral particles induce acute gastroenteritis [2, 14]. Because it is thought that MNV also has strong infectivity the virus needs to be inactivated as completely possible to prevent the spread of MNV. PVP-I, which showed strong virucidal activity in a short time frame against MNV, would be useful for preventing MNV transmissions by human hand washing in laboratories.

In this study, we found that the results of quantitative RT-PCR were not consistent with those of the virucidal assay (Table 1), and the detection of viral RNA was not necessarily related to the virus titers, demonstrating the importance of conducting infectivity assays when evaluating the efficacy of antiseptics. The efficacy of antiseptics may be underestimated if quantitative RT-PCR is used for evaluation, as reported in a previous paper [1]. Thus, interpretation of the results of quantitative

RT-PCR needs further consideration.

In conclusion, our data demonstrate that a novel MNV isolate, MT30-2, is a useful tool to evaluate the effectiveness of antiseptics and that PVP-I as well as NaOCl is the most effective antiseptics for disinfection and infection control of MNV.

References

1. Belliot, G., Lavaux, A., Souihel, D., Agnello, D., and Pothier, P. 2008. Use of murine norovirus as a surrogate to evaluate resistance of human norovirus to disinfectants. 2008. *Appl. Environ. Microbiol.* 74: 3315–3318.
2. Cremon, C., De Giorgio, R., and Barbara, G. 2010. Norovirus gastroenteritis. *N. Engl. J. Med.* 361: 1776–1785.
3. Doultree, J.C., Druce, J.D., Birch, C.J., Bowden, D.S., and Marshall, J.A. 1999. Inactivation of feline calicivirus, a Norwalk virus surrogate. *J. Hosp. Infect.* 41: 51–57.
4. Duizer, E., Bijkerk, P., Rockx, B., De Groot, A., Twisk, F., and Koopmans, M. 2004. Inactivation of caliciviruses. *Appl. Environ. Microbiol.* 70: 4538–4543.
5. Duizer, E., Schwab, K.J., Neill, F.H., Atmar, R.L., Koopmans, M.P., and Estes, M.K. 2004. Laboratory efforts to cultivate noroviruses. *J. Gen. Virol.* 85: 79–87.
6. Goto, K., Hayashimoto, N., Yasuda, M., Ishida, T., Kameda, S., Takakura, A., and Itoh, T. 2009. Molecular detection of murine norovirus from experimentally and spontaneously infection mice. *Exp. Anim.* 58: 135–140.
7. Hsu, C.C., Riley, L.K., Wills, H.M., and Livingston, R.S. 2006. Persistent infection with and serologic cross-reactivity of three novel murine noroviruses. *Comp. Med.* 56: 247–251.
8. Hsu, C.C., Wobus, C.E., Steffen, E.K., Riley, L.K., and Livingston, R.S. 2005. Development of a microsphere-based serologic multiplexed fluorescent immunoassay and a reverse transcriptase PCR assay to detect murine norovirus 1 infection in mice. *Clin. Diagn. Lab. Immunol.* 10: 1145–1151.
9. Karst, S.M., Wobus, C.E., Lay, M., Davidson, M., and Virgin, H.W. 2003. STAT 1-dependent innate immunity to a Norwalk-like virus. *Science* 299: 1575–1578.
10. Kawana, R., Kitamura, T., Nakagomi, O., Matsumoto, I., Arita, M., Yoshihara, N., Yanagi, K., Yamada, A., Morita, O., Yoshida, Y., Furuya, Y., and Chiba, S. 1997. Inactivation of human viruses by povidone-iodine in comparison with other antiseptics. *Dermatology* 195: 29–35.
11. Lages, S.L., Ramakrishnan, M.A., and Goyal, S.M. 2008. In-vivo efficacy of hand sanitisers against feline calicivirus: a surrogate for norovirus. *J. Hosp. Infect.* 68: 159–163.
12. Maler, M. and Kol, W. 2009. A serological survey to evaluate contemporary prevalence of viral agents and Mycoplasma pulmonis in laboratory mice and rats in western Europe. *Lab. Anim. (NY)* 38: 161–165.
13. Mumphrey, S.M., Changotra, H., Moore, T.N., Heimann-Nichols, E.R., Wobus, C.E., Reilly, M.J., Moghadamfalahi, M., Shukla, D., and Karst, S.M. 2007. Murine norovirus 1 infection is associated with histopathological changes in immunocompetent hosts, but clinical disease is prevented by STAT1-dependent interferon responses. *J. Virol.* 81: 3251–3263.
14. Teunis, P.F., Moe, C.L., Liu, P., Miller, S.E., Lindesmith, L., Baric, R.S., Le Pendu, J., and Calderon, R.L. 2008. Norwalk virus: how infectious is it? *J. Med. Virol.* 80: 1468–1476.
15. Thackray, L.B., Wobus, C.E., Chachu, K.A., Liu, B., Alegre, E.R., Henderson, K.S., Kelley, S.T., and Virgin, H.W. 2007. Murine noroviruses comprising a single genogroup exhibit biological diversity despite limited sequence divergence. *J. Virol.* 81: 10460–10473.
16. Urakami, H., Ikarashi, K., Okamoto, K., Abe, Y., Ikarashi, T., Kono, T., Konagaya, Y., and Tanaka, N. 2007. Chlorine sensitivity of feline calicivirus, a norovirus surrogate. *Appl. Environ. Microbiol.* 73: 5679–5682.
17. Wobus, C.E., Thackray, L.B., and Virgin, H.W. 2006. Murine norovirus: a model system to study norovirus biology and pathogenesis. *J. Virol.* 80: 5104–5112.
18. Wobus, C.E., Karst, S.M., Thackray, L.B., Chang, K.O., Sosnovtsev, S.V., Belliot, G., Krug, A., Mackenzie, J.M., Green, K.Y., and Virgin, H.W. 2004. Replication of norovirus in cell culture reveals a tropism for dendritic cells and macrophages. *PLoS Biol.* 2: 2076–2084.

Arch Virol (2012) 157:349–352
DOI 10.1007/s00705-011-1161-2

BRIEF REPORT

Human sapovirus classification based on complete capsid nucleotide sequences

Tomoichiro Oka · Kohji Mori · Nobuhiro Iritani · Seiya Harada · You Ueki · Setsuko Iizuka · Keiji Mise · Kosuke Murakami · Takaji Wakita · Kazuhiko Katayama

Received: 19 August 2011 / Accepted: 7 October 2011 / Published online: 11 November 2011

Abstract The genetically diverse sapoviruses (SaVs) are a significant cause of acute human gastroenteritis. Human SaV surveillance is becoming more critical, and a better understanding of the diversity and distribution of the viral genotypes is needed. In this study, we analyzed 106 complete human SaV capsid nucleotide sequences to provide a better understanding of their diversity. Based on those results, we propose a novel standardized classification scheme that meets the requirements of the International Calicivirus Scientific Committee. We believe the classification scheme and strains described here will be of value for the molecular characterization and classification of newly detected SaV genotypes and for comparing data worldwide.

Sapoviruses (SaVs) cause gastroenteritis in humans and are a significant public-health problem. Numerous studies have documented their importance in outbreaks of sporadic gastroenteritis and in contaminated food destined for human consumption [1, 3, 7, 8, 10–12, 16–19, 21, 23].

The SaV genome is a positive-sense, nonsegmented single-strand RNA molecule of approximately 7.5 kb that is polyadenylated at the 3′ terminus. The SaV genome contains two or three open reading frames (ORFs). ORF1 encodes non-structural proteins (i.e., VPg, protease, and RNA-dependent RNA polymerase [RdRp]) and a capsid protein (VP1). ORF2 and ORF3 encode proteins of unknown function. The capsid protein is thought to contain all of the determinants for viral attachment and antigenicity [2, 5].

The most widely used method of human SaV detection is reverse transcription–PCR (RT-PCR). It has high sensitivity and can be used to analyze the virus genetically [9, 16, 17, 20, 22]. Real-time RT-PCR is also used to detect the virus. It is highly sensitive and useful for quantitative analysis [14]. Direct serotyping based on neutralization is not possible for human SaVs because no cell-culture system supporting SaV replication has been established.

T. Oka (✉) · K. Murakami · T. Wakita · K. Katayama
Department of Virology II, National Institute of Infectious Diseases, Gakuen 4-7-1, Musashimurayama-shi, Tokyo 208-0011, Japan
e-mail: oka-t@nih.go.jp

T. Oka
Food Animal Health Research Program, Ohio Agricultural Research and Development Center, Department of Veterinary Preventive Medicine, The Ohio State University, Wooster, OH 44691, USA

K. Mori
Tokyo Metropolitan Institute of Public Health, Tokyo, Japan

N. Iritani
Osaka City Institute of Public Health and Environmental Sciences, Osaka, Japan

S. Harada
Kumamoto Prefectural Institute of Public Health and Environmental Science, Kumamoto, Japan

Y. Ueki
Miyagi Prefectural Institute of Public Health and Environment, Miyagi, Japan

S. Iizuka
Shimane Prefectural Institute of Public Health and Environmental Science, Shimane, Japan

K. Mise
Sapporo Medical University Center for Medical Education, Hokkaido, Japan

From the sequence data for complete capsids, human SaVs are a genetically diverse group [4]. At least four different human SaV genogroups and numerous genotypes have been described, and for the most part, the antigenicity corresponds well to the genetic classification [6, 15]. However, many molecular epidemiological studies have relied on only partially sequenced genes because the broadly reactive RT-PCR primer sets for the SaV capsid-encoding region were directed against highly conserved regions [16, 17, 22]. The International Calicivirus Scientific Committee at the Fourth International Conference on Caliciviruses in Chile (in 2010) proposed that new norovirus and SaV genotypes should only be named after the complete capsid sequence (approximately 1700 nt in length) is determined and compared to other complete capsid sequences. A standardized genotyping and nomenclature system based on appropriate criteria is necessary to facilitate worldwide comparison of data.

In this study, we have analyzed the nucleotide sequences of 107 complete SaV capsids (106 human SaVs and one porcine SaV). Ninety-one human SaV and one porcine SaV sequences were collected from the calicivirus database (http://teine.cc.sapmed.ac.jp/~calici/ddbj/) on February 23, 2011. The sequences of 16 additional human SaVs from gastroenteritis patients in five prefectures of Japan were newly determined by PCR-based direct sequencing as described [11, 12] and deposited in the DDBJ/Genbank/EMBL database under the following accession numbers: AB429084, AB522390–AB522392, AB622429, AB622432, AB622435–AB622439, AB622441, AB623037, AB630067, AB630068, and AB630340. The nucleic acid sequences were aligned with ClustalW (version 1.83), and the gaps were removed. The genetic distances were calculated using the Kimura's two-parameter method, and a distance matrix file was created (http://clustalw.ddbj.nig.ac.jp/top-j.html). These data were used to generate histograms of the relative frequency distributions of pairwise distance values (Graph Pad Prism version 4.0). The phylogenetic tree with 1000 bootstrap replicates was generated by the neighbor-joining (NJ) method using Clustal W (version 1.83) and was drawn with NJplot software (http://pbil.univ-lyon1.fr/software/njplot.html).

The frequency histogram of pairwise distance values with 107 SaV complete capsid nucleotide sequences resulted in three clearly distinct and non-overlapping symmetrical peaks (0–0.112 [mean 0.036], 0.153–0.414 [mean 0.290], and 0.606–0.872 [mean 0.683]) (Fig. 1). These three peaks were considered to represent the strain, genotype, and genogroup, respectively. The mean ± 3SD of each pairwise distance value for strain, genotype, and genogroup were 0–0.127, 0.201–0.379, and 0.562–0.803, respectively (Fig. 1). The cutoff values for the genotype and genogroup clusters were <0.200 and <0.561, respectively. A phylogenetic tree of the 107 SaV complete capsid nucleotide sequences was constructed by the NJ method (Fig. 2). SaV was divided into five genogroups, GI, GII, GIII, GIV, and GV, among which human SaV were classified into GI, GII, GIV, and GV. SaV GI and GII were each subdivided into seven genotypes, and GIV and GV were placed into a single genotype by the distance criteria as described above. The genotype numbers were assigned consecutively as shown in Fig. 2.

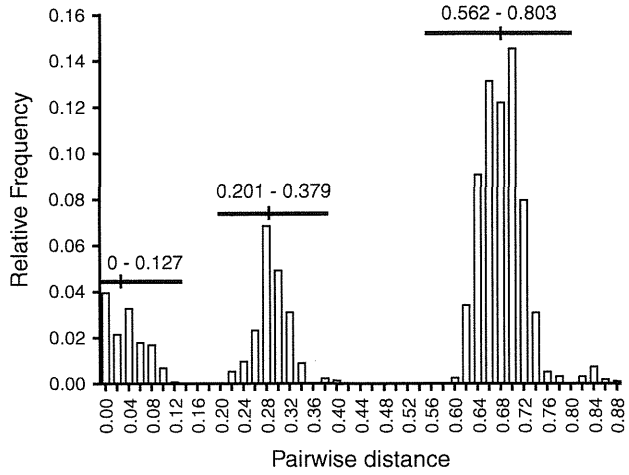

Fig. 1 Pairwise distance distribution of 107 SaV strains using the entire capsid nucleotide sequences. The horizontal bars indicates the mean value ± 3 SD for each distribution peaks of strain, genotype, and genogroup, respectively

Recent experiments with virus-like particles (VLPs) have demonstrated the different antigenicities among the GI, GII, GIV, and GV strains [6], and between GI.1 vs GI.5 [6, 7], and GII.2 vs GII.3 strains [15]. Therefore, a classification scheme based on the complete capsid sequence might well reflect the antigenic phenotype of SaV and can also be useful for selecting representative strains for preparing VLPs or VP1 panels for further immunological studies.

In conclusion, we provide a novel human SaV classification based on complete capsid gene sequences. Our classification scheme is based on statistically defined cutoff pairwise distance values. This classification method will aid in the molecular characterization and classification of newly detected SaV genotypes. Recently, a web-based automated genotyping tool for noroviruses was established by the National Institute for Public Health and the Environment and Centers for Disease Control and Prevention [13]. As the number of SaV surveillance laboratories appears to be increasing, a similar web-based genotyping tool with the reference nucleotide sequence sets described in this study will also be valuable for SaV data comparison.

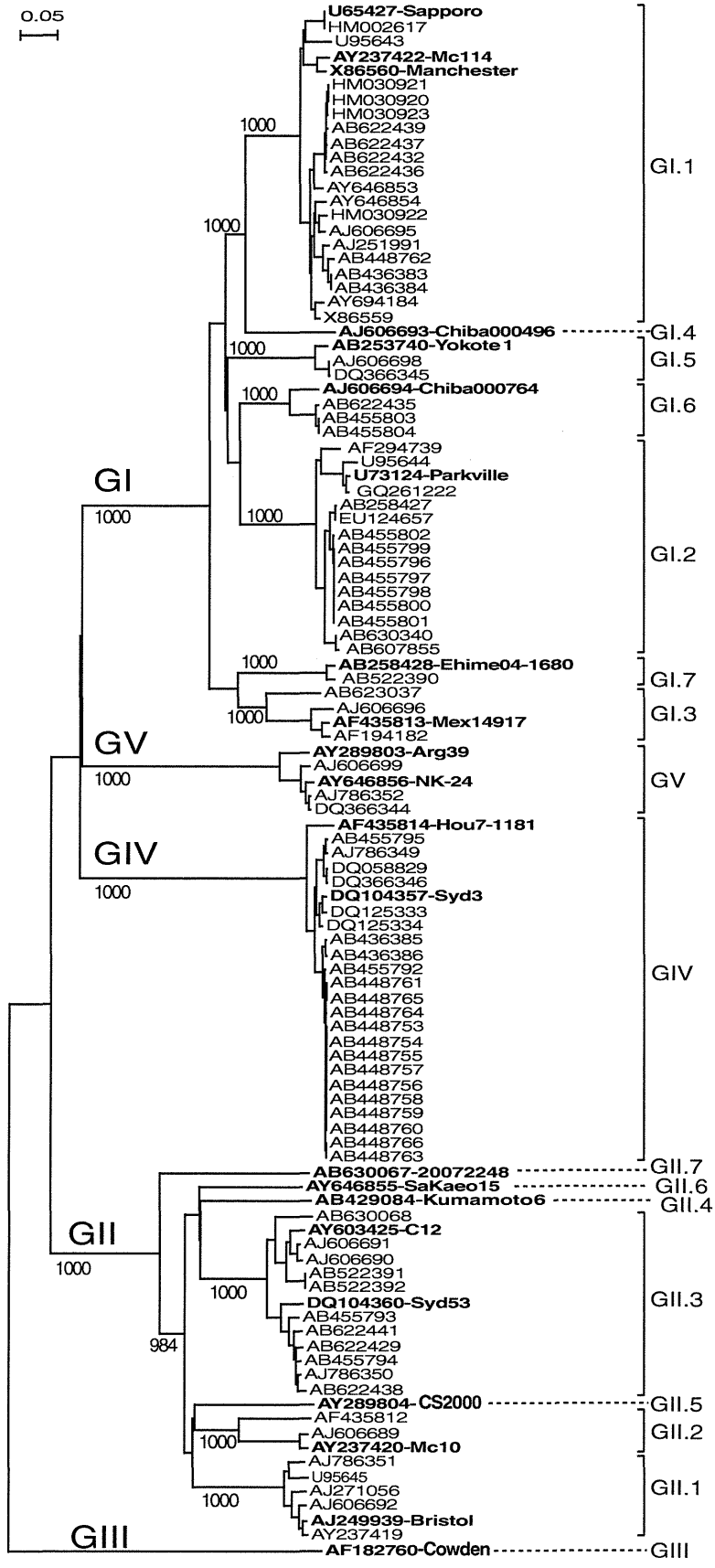

Fig. 2 Phylogenetic trees constructed using the entire capsid nucleotide sequences of 107 SaV strains. The accession numbers and assigned genogroup and genotypes are indicated. Representative strain(s) of each genogroup or genotype are indicated in boldface type. The bootstrap values correspond to 1000 replications. The number on each branch indicates the bootstrap value, where a value higher than 950 is indicated. The scale represents nucleotide substitutions per site

Acknowledgments This work was supported in part by grants for Research on Emerging and Re-emerging Infectious Diseases, as well as Research on Food Safety, from the Ministry of Health, Labour, and Welfare of Japan. We thank Mineyuki Okada for his assistance in sequencing and database submission.

References

1. Akihara S, Phan TG, Nguyen TA, Yagyu F, Okitsu S, Muller WE, Ushijima H (2005) Identification of sapovirus infection among Japanese infants in a day care center. J Med Virol 77:595–601
2. Clarke IN, Lambden PR (2000) Organization and expression of calicivirus genes. J Infect Dis 181(Supp 2):S309–S316
3. Dey SK, Phan TG, Nguyen TA, Nishio O, Salim AF, Yagyu F, Okitsu S, Ushijima H (2007) Prevalence of sapovirus infection among infants and children with acute gastroenteritis in Dhaka City, Bangladesh during 2004–2005. J Med Virol 79:633–638
4. Farkas T, Zhong WM, Jing Y, Huang PW, Espinosa SM, Martinez N, Morrow AL, Ruiz-Palacios GM, Pickering LK, Jiang X (2004) Genetic diversity among sapoviruses. Arch Virol 149: 1309–1323
5. Green KY (2007) Caliciviridae: the Noroviruses. In: Knipe DM, Howley PM, Griffin DE, Lamb RA, Martin MA, Roizman B, Straus SE (eds) Fields Virology, 5th edn. Lippincott Williams & Wilkins, Philadelphia, pp 949–979
6. Hansman GS, Oka T, Sakon N, Takeda N (2007) Antigenic diversity of human sapoviruses. Emerg Infect Dis 13:1519–1525
7. Hansman GS, Saito H, Shibata C, Ishizuka S, Oseto M, Oka T, Takeda N (2007) Outbreak of gastroenteritis due to sapovirus. J Clin Microbiol 45:1347–1349
8. Harada S, Okada M, Yahiro S, Nishimura K, Matsuo S, Miyasaka J, Nakashima R, Shimada Y, Ueno T, Ikezawa S, Shinozaki K, Katayama K, Wakita T, Takeda N, Oka T (2009) Surveillance of pathogens in outpatients with gastroenteritis and characterization of sapovirus strains between 2002 and 2007 in Kumamoto Prefecture, Japan. J Med Virol 81:1117–1127
9. Honma S, Nakata S, Sakai Y, Tatsumi M, Numata-Kinoshita K, Chiba S (2001) Sensitive detection and differentiation of Sapporo virus, a member of the family Caliciviridae, by standard and booster nested polymerase chain reaction. J Med Virol 65: 413–417
10. Iizuka S, Oka T, Tabara K, Omura T, Katayama K, Takeda N, Noda M (2010) Detection of sapoviruses and noroviruses in an outbreak of gastroenteritis linked genetically to shellfish. J Med Virol 82:1247–1254
11. Ishida S, Yoshizumi S, Miyoshi M, Ikeda T, Okui T, Katayama K, Takeda N, Oka T (2008) Characterization of sapoviruses detected in Hokkaido, Japan. Jpn J Infect Dis 61:504–506
12. Iwakiri A, Ganmyo H, Yamamoto S, Otao K, Mikasa M, Kizoe S, Katayama K, Wakita T, Takeda N, Oka T (2009) Quantitative analysis of fecal sapovirus shedding: identification of nucleotide substitutions in the capsid protein during prolonged excretion. Arch Virol 154:689–693
13. Kroneman A, Vennema H, Deforche K, v d Avoort H, Penaranda S, Oberste MS, Vinje J, Koopmans M (2011) An automated genotyping tool for enteroviruses and noroviruses. J Clin Virol 51:121–125
14. Oka T, Katayama K, Hansman GS, Kageyama T, Ogawa S, Wu FT, White PA, Takeda N (2006) Detection of human sapovirus by real-time reverse transcription-polymerase chain reaction. J Med Virol 78:1347–1353
15. Oka T, Miyashita K, Katayama K, Wakita T, Takeda N (2009) Distinct genotype and antigenicity among genogroup II sapoviruses. Microbiol Immunol 53:417–420
16. Okada M, Shinozaki K, Ogawa T, Kaiho I (2002) Molecular epidemiology and phylogenetic analysis of Sapporo-like viruses. Arch Virol 147:1445–1451
17. Okada M, Yamashita Y, Oseto M, Shinozaki K (2006) The detection of human sapoviruses with universal and genogroup-specific primers. Arch Virol 151:2503–2509
18. Pang XL, Lee BE, Tyrrell GJ, Preiksaitis JK (2009) Epidemiology and genotype analysis of sapovirus associated with gastroenteritis outbreaks in Alberta, Canada: 2004–2007. J Infect Dis 199:547–551
19. Svraka S, Vennema H, van der Veer B, Hedlund KO, Thorhagen M, Siebenga J, Duizer E, Koopmans M (2010) Epidemiology and genotype analysis of emerging sapovirus-associated infections across Europe. J Clin Microbiol 48:2191–2198
20. Vinje J, Deijl H, van der Heide R, Lewis D, Hedlund KO, Svensson L, Koopmans MP (2000) Molecular detection and epidemiology of Sapporo-like viruses. J Clin Microbiol 38:530–536
21. Yamashita Y, Ootsuka Y, Kondo R, Oseto M, Doi M, Miyamoto T, Ueda T, Kondo H, Tanaka T, Wakita T, Katayama K, Takeda N, Oka T (2010) Molecular characterization of Sapovirus detected in a gastroenteritis outbreak at a wedding hall. J Med Virol 82:720–726
22. Yan H, Yagyu F, Okitsu S, Nishio O, Ushijima H (2003) Detection of norovirus (GI, GII), Sapovirus and astrovirus in fecal samples using reverse transcription single-round multiplex PCR. J Virol Methods 114:37–44
23. Yoshida T, Kasuo S, Azegami Y, Uchiyama Y, Satsumabayashi K, Shiraishi T, Katayama K, Wakita T, Takeda N, Oka T (2009) Characterization of sapoviruses detected in gastroenteritis outbreaks and identification of asymptomatic adults with high viral load. J Clin Virol 45:67–71

frontiers in
MICROBIOLOGY

PERSPECTIVE ARTICLE
published: 06 November 2012
doi: 10.3389/fmicb.2012.00387

In silico 3D structure analysis accelerates the solution of a real viral structure and antibodies docking mechanism

Motohiro Miki[1,2] and Kazuhiko Katayama[1]*

[1] Department of Virology II, National Institute of Infectious Diseases, Tokyo, Japan
[2] Denka-Seiken Co., Ltd, Niigata, Japan

Edited by:
Hironori Sato, National Institute of Infectious Diseases, Japan

Reviewed by:
Masaru Yokoyama, National Institute of Infectious Diseases, Japan
Sam-Yong Park, Yokohama City University, Japan

***Correspondence:**
Kazuhiko Katayama, Department of Virology II, National Institute of Infectious Diseases, Tokyo 208-0011, Japan.
e-mail: katayama@nih.go.jp

Norwalk virus (NoV) is responsible for most outbreaks of non-bacterial gastroenteritis. NoV is genetically diverse and show antigenically variable. Recently, we produced a monoclonal antibody called 5B-18 that reacts broadly with NoV genogroup II (GII). We suspected the 5B-18 binds to a conformational epitope on 3D structure of virion. X-ray crystallography showed us that 5B-18 binds to NoV at the P domain, which protrudes from the capsid surface of the virion. However, there seems to be no space that would allow the IgG to approach the virion. To solve this problem, we used cryo-electron microscopy to examine NoV GII virus-like particles (VLPs). The P domain rises up higher in NoV GII than in NoV GI, and it seems to form an outer layer around the virion. Finally, using *in silico* modeling we found the 5B-18 Fab arms and NoV P region are quite flexible, so that 5B-18 can bind the NoV virion from bottom of P domain. This study demonstrates the shortcomings of studying biological phenomenon by only one technique. Each method has limitations. Multiple methods and modeling *in silico* are the keys to solving structural problems.

Keywords: Norwalk virus, monoclonal antibody, x-ray crystallography, *in silico* modeling, cryo-electron microscopy

THE BASICS OF NORWALK VIRUS

Norwalk virus (NoV) is responsible for most of the outbreaks of non-bacterial gastroenteritis in developed countries and, it is thought, in developing countries as well. Yet, although NoV was identified more than 30 years ago, we know little about their pathogenicity and basic virology (Guix et al., 2007). Studies of NoV have been hampered by the lack of a cell-culture system or a small animal model in which the virus will grow, except murine norovirus that is classified as NoV genogroup V (Wobus et al., 2006).

NoV belongs to the family Caliciviridae. The genus *Norovirus* has only one species, *Norwalk viruses*, with five genogroups (GI–GV). Genogroup GI and II cause most human infections, and they are further subdivided into numerous genotypes (GI.1–8 and GII.1–17; Zheng et al., 2006). The NoV genome is a 7.3 to 7.7-kb positive-sense, polyadenylated, single-stranded RNA molecule. It contains three open reading frames (ORFs): ORF1 encodes a non-structural polyprotein, and ORF2 and ORF3 encode the major and minor capsid proteins, VP1 and VP2, respectively (Jiang et al., 1992; Lambden et al., 1993).

Without an *in vitro* system for propagating the virus, the antigenicity of NoV has been inferred from studies of virus-like particles (VLPs). Nucleic acid-free VLPs self-assemble when the capsid protein is expressed in a baculovirus expression system (**Figure 1A**). The VLPs are assumed to have a similar morphology and, thus, antigenicity as that of the native virions (Jiang et al., 1992). Cryo-electron microscopy (cryo-EM) and x-ray crystal structures of the prototype norovirus VLP (GI.1, Norwalk virus) showed that the VLPs form a T = 3 icosahedral structure (Prasad et al., 1994, 1999).

However, structures of large protein complexes are difficult to determine by x-ray analysis. We sought to understand the structure of the virion and how it interacts with antibodies by combining data from x-ray diffraction, cryo-EM, and *in silico* modeling.

A MONOCLONAL ANTIBODY REACTS BROADLY WITH NoV GII

NoV is generally detected by RT-PCR with degenerate primers or an ELISA with NoV-specific antibodies. Many polyclonal and monoclonal antibodies used in the ELISA kits were developed in mice or rabbit immunized with norovirus VLPs (Hansman et al., 2011).

Recently, we produced a monoclonal antibody called 5B-18 that reacts broadly with NoV GII (Hansman et al., 2012). In fact, 5B-18 is used as a NoV GII broad-range capture antibody in a commercial ELISA kit [NV-AD(III) SEIKEN NoV antigen ELISA] and in an immunochromatography (IC) kit (Quick naviNoro IC kit, both from Denka-Seiken, Japan).

The 5B-18 monoclonal antibody was produced by immunizing a mouse with norovirus VLPs. Several monoclonal antibodies bind to the shell (S) domain (Yoda et al., 2003; Li et al., 2010), and others bind to the protruding (P) domain (Lindesmith et al., 2012). We suspect that 5B-18 also binds to S or P domain on the surface of the NoV virion. However, no high-resolution structural details of the antibody binding to the VLPs, S domain or P domain are available.

X-RAY CRYSTALLOGRAPHY OF THE BINDING SITE

The 5B-18 binds major NoV genotypes, such as GII.4 and GII.3, and the minor NoV genotypes GII.10 and GII.12 strongly. We suspect 5B-18 binds to a conserved epitope on the NoV capsid surface. We wanted to define the recognition site of 5B-18 and the NoV minor genotype GII.10 P domain, and we began with x-ray

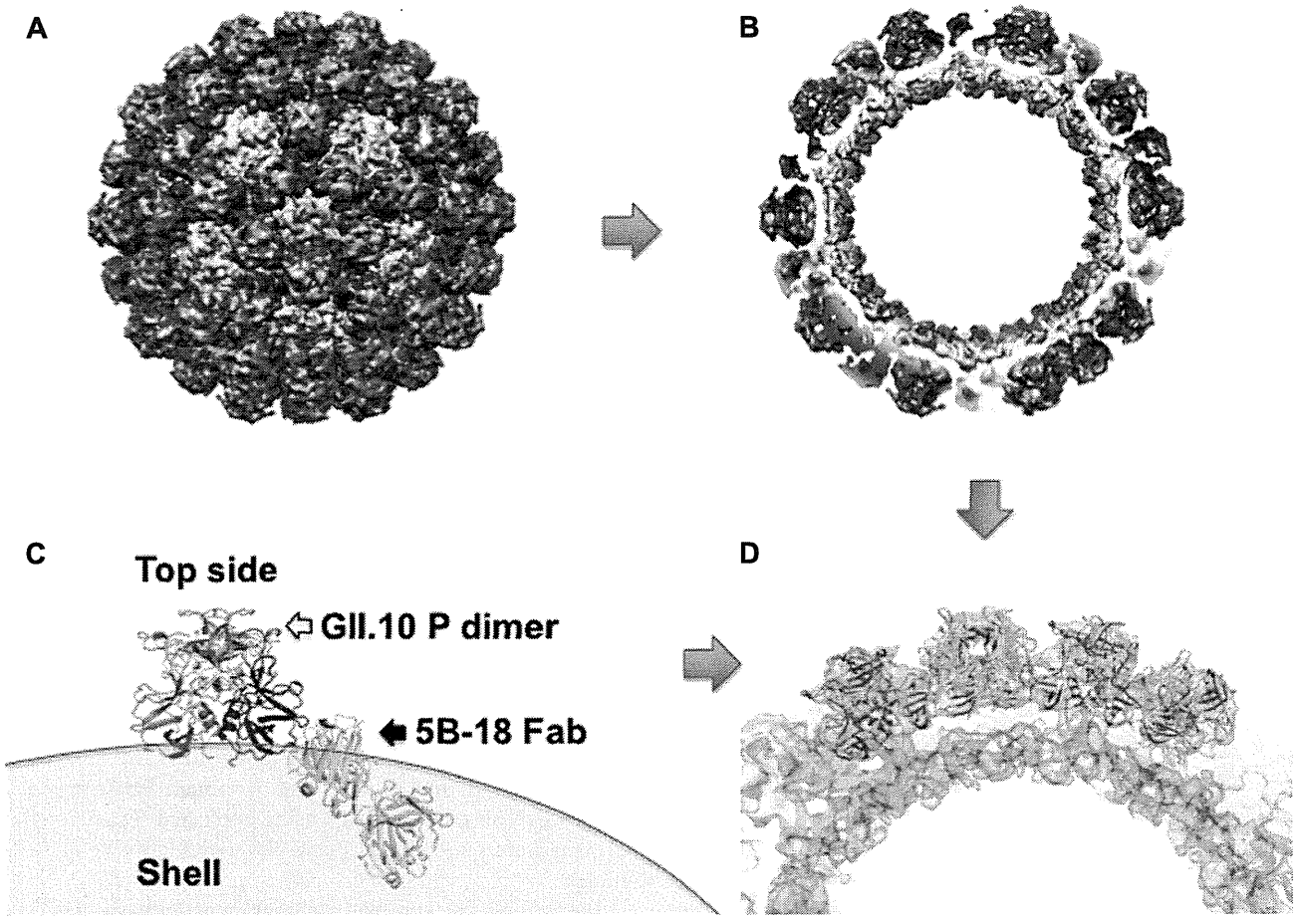

FIGURE 1 | The cryo-EM image of GII.10 VLP and the P dimer structure fit to the cryo-EM image by *in silico* modeling. The cryo-EM structure of NoV GII.10 VLP was constructed with 180 molecules of VP1 protein **(A)**. The cross-section of GII.10 VLP **(B)**. P domains (blue and green) rise up from shell domain (yellow), and it seemed to construct an outer layer of the capsid. Diagram based on the x-ray crystal structure of the GII.10 P domain-Fab complex shows Fab bound to the lower side of the P1 sub domain. Top side indicates the outside of the VLP, and the shell side contains the VLP core that is called shell. A white arrow indicates the GII.10 P dimer; the monomer is colored blue and purple. Black arrow shows MoAb 5B-18 Fab region. Green represents the heavy chain, and yellow represents the kappa chain. The part of oval shadow represents VLP shell **(C)**. The x-ray crystallography was fit into the cryo-EM structure by *in silico* modeling **(D)**. The GII.10 P domain (apo P domain structure) into the A/B dimer subunit (light blue and pink, respectively) and C/C dimer subunit (cyan).

crystallography, one of the gold standard for protein structural studies. We expressed the NoV GII.10 P domain in the *Escherichia coli* strain BL21 (DE3). The P domain was purified and stored in gel filtration buffer. Next we prepared of 5B-18 Fab fragment by immunizing a mouse with NoV GII.4-strain 445 VLPs (GenBank accession number DQ093064; Denka-Seiken, Japan). To prepare crystals of the bound complex, purified GII.10 P domain and Fab were mixed in a 1.4:1 ratio. Crystals were grown by the hanging-drop vapor-diffusion method, mixing the protein and reservoir solution (40% [vol/vol] polyethylene glycol [PEG] 400, 5% [wt/vol] PEG 3350, and 0.1 M acetic acid, pH 5.5) in a 1:1 ratio. Crystals grew over 1 week at 20°C.

One GII.10 P domain-Fab complex crystal diffracted x-rays to a resolution 3.3Å, and we solved the structure by molecular replacement with a GII.10 P domain monomer (PDB ID 3ONU) and a mouse Fab (PDB ID 1WEJ) as search models. Molecular replacement indicated an asymmetrical unit contained two P domain monomers and two 5B-18 Fabs, each with a kappa and a heavy chain (**Figure 1C**; Hansman et al., 2012).

The binding of the P domain and the Fab involved nine hydrogen bonds. Of these, eight linked the P1 subdomain to the kappa chain, and one linked the P1 subdomain and the heavy chain. More specifically, the amino acids in the P1 subdomain amino acids that interacted with the 5B-18 Fab were as follows (in each pair, the amino acids are for the P1 domain and Fab, respectively): Tyr533 and Tyr92 (one bond), Thr534 and Gly93 (three bonds), Thr534 and Trp97 (one bond), Leu535 and Tyr32 (one bond), Glu496 and Tyr92 (one bond), and Asn530 and Ser94 (one bond). Finally, Val433 and Asn52 in the heavy chain formed one hydrogen bond (Hansman et al., 2012).

CONFIRMATION OF 5B-18 BINDING

With the x-ray crystallographic analysis, we found the 5B-18 antibody bound to a hidden site on the P domain that is located inside

of the shell of NoV particle. However, in a previous study, the NoV GI structure indicated that bottom of the P domain was completely covered by the shell of NoV particle (**Figure 1C**). If the structure of GII is the same as GI, then 5B-18 could not bind GII. These results presented an apparent paradox for the 5B-18 binding mechanism. To resolve the paradox, we set out to identify the binding residue in the capsid.

From the crystallographic analysis, we knew that the 5B-18 Fab formed hydrogen bonds with residues at three sites in the P1 subdomain, called A, B, and C (**Figure 2A**). By aligning the amino acid sequences of representatives from NoV GII genotypes, we discovered that Val433 (site A) was the most variable. Other genotypes had threonine, serine, asparagine, leucine, or methionine at this position. Thr534 (site C) was mostly conserved: the only other amino acid at this position was a serine. Glu496 (site B), Asn530 (site C), Tyr533 (site C), and Leu535 (site C) were all highly conserved among the representative GII genotypes.

To confirm that 5B-18 binds the A, B, and C regions, we divided the GII.10 capsid domain into three major subdomains: N, S, P1-1 P2, and P1-2. We prepared five constructs (1–5), expressed them in an *E. coli* expression system, and identified a liner epitope of 5B-18 by western blotting (**Figure 2B**). Construct 3, a P1-2 region (i.e., A, B, and C), showed the strongest band signal, and construct 5 (i.e., B and C) showed a positive band. The intensity of the band from construct 5 was only about half the strength of construct 3 because it did not contain epitope A. However, construct 4 included only A, and constructs 1 and 2 also were not detected. Thus, the three 5B-18 epitopes A, B, and C were confirmed to be part of the binding epitope.

Next, we determined if 5B-18 binds to other NoV GII VLPs (**Figure 2A**). We prepared and purified six kinds of GII VLPs that were 809 (GII.3), 104 (GII.4), 445 (GII.6), 026 (GII.10), Hiro (GII.12), and GII.13 VLPs as aligned in **Figure 2A**. The GII VLPs that had all 5B-18 epitopes A, B, and C were captured by the anti-GII VLPs rabbit serum that was pre-coated on ELISA plate and detected with 5B-18 and horseradish peroxidase (HRP)-labeled anti-mouse IgG secondary antibodies. When the cut-off value was under 0.2, 5B-18 detected all kinds of GII VLPs in a dose-dependent manner (data not shown). These results suggested that 5B-18 binds to a variety of GII VLPs. In fact, the commercial ELISA and IC kits use 5B-18 (Denka-Seiken, Japan), and we have practical results showing that 5B-18 detects various infectious NoV GII in stool samples.

COMBINING CRYO-EM AND *IN SILICO* MODELING TO SOLVE A PARADOX

We had a simple question. Are the structures of NoV GI VLP and GII VLP the same or not? For G1 VLP, there is no space where the 5B-18 can access and bind the bottom of P domain. If the GII VLP had same conformation as the GI VLP, the lower part of the P domain would be buried under the virion shell (**Figure 1C**). However, 5B-18 binds and detects GII VLPs and GII infectious viruses. These conflicting facts suggested that the structures of the GII VLPs and infectious GII virions were different than the GI VLP structure. However, structure determinations by x-ray crystallography have many challenges and limitations, and we suspected this might be one of those cases.

To answer the question, we turned to cryo-EM and *in silico* modeling. We reconstructed the overall structure of GII.10 VLPs and 5B-18 Fabs from the x-ray structural data. To determine if the GII VLP had enough space to allow binding, we also used *in silico* modeling to fit the P and 5B-18 Fabs structures that had been derived by x-ray crystallography.

The GII.10 VLPs formed homogeneous, monodisperse particles in ice. By reference-free class averages and at 10Å resolution (0.5 FSC criterion), these icosahedral particles had several notable features, including spike-like structures extending from the vertices (**Figure 1B**), and at the three- and fivefold axes, significant amounts of the surface of the S domain were exposed (**Figure1A**). The GII.10 VLP P domain formed a second outer shell that seems to be separated from the S domain by about 15Å (**Figure 1B**). Thus, unlike the GI VLPs and virions, GII VLPs and virions seem to have a space between the shell and bottom of P domain, indicating that the two genotypes have different structures. Furthermore, the electron density was much weaker at the tip of the P domain (the P2 subdomain) than at the base. This observation is consistent with published reconstructions of calicivirus particles (Bhella et al., 2008; Bhella and Goodfellow, 2011) and indicates that the P domains have considerable heterogeneity.

Next we attempted to fit the GII.10 P domain and P domain-Fab complex structures into the GII.10 VLP cryo-EM structure. At 10Å resolution, the GII.10 P domain monomers in the VLP were easily distinguished. We manually fitted the crystal structures of the GII.10 P domain and P domain-Fab complex into the GII.10 VLP cryo-EM map, using published reports of GV.1 P domain dimers and the GV.1 cryo-EM map (Taube et al., 2010) as guides.

We refined the approximate alignment with the Fit-in-Map function in UCSF Chimera (Pettersen et al., 2004) to a cross-correlation coefficient of 0.94 (**Figure 1D**) with excellent results. The x-ray structure of the GII.10 P domain dimer (PDB ID 3ONU) unambiguously fitted the corresponding density in the cryo-EM map (**Figure 1D**). Only some loops of the P2 subdomain did not fit. They had only weak electron density, and their tips were less ordered than the S domain and P1 domains in the cryo-EM reconstruction. These subdomains are probably more flexible. P1, but not the P2, subdomains in the VLP appeared to be connected to the P domain dimers.

Next we fitted the x-ray structure of the P domain from the P domain-Fab complex into the reconstructed A/B dimer subunit and found that the 5B-18 binding site was close to an adjacent dimer of P domain (**Figure 1C**). At the twofold axes, the 5B-18 Fab was hindered by the S domain, which also provided an obstacle to assembly of the neighbor P domain dimer. However, when the P domain was fitted into the C/C dimer subunit, the 5B-18 Fab was in contact with the P domain dimer and slightly interfered with part of the S domain at the fivefold axes. Thus, the antibody binding site overlapped with part of the P1 subdomain.

Thus, this model predicted an unstable structure in which the VLP could not bind with the 5B-18 antibodies. How could this be? There are several possibilities. First, 5B-18 might bind at sites on the P domain that are only transiently exposed. Second, 5B-18 might bind to defects in the P domain. Finally, the Fab arms of 5B-18 might be very flexible.

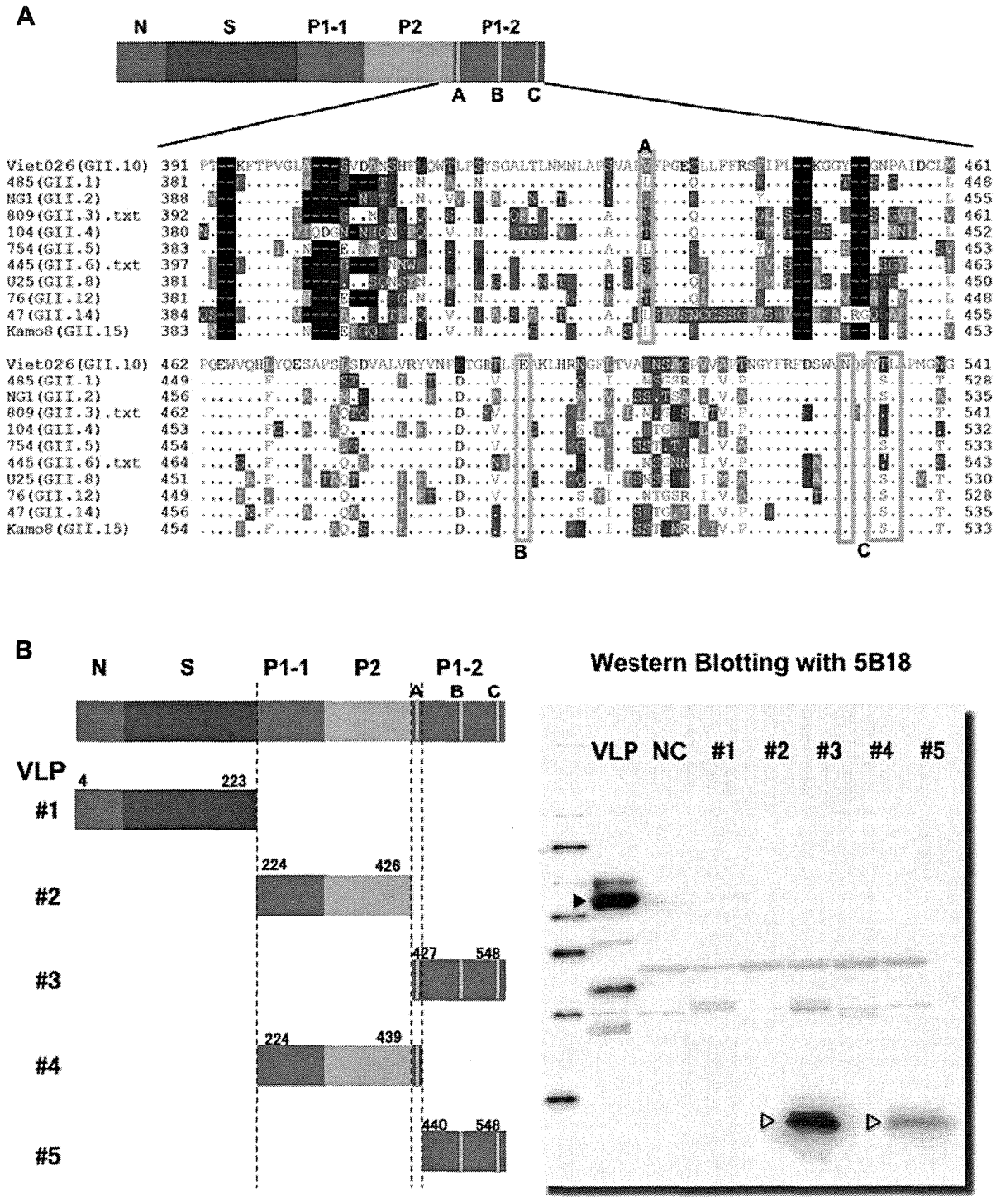

FIGURE 2 | Schematic diagram of NoV VP1 protein and the amino acid alignment of NoV GII VP1 sequences. Capsid (VP1) sequences from 11 GII genotypes were aligned, and the GII.10 capsid sequence was used as the consensus. The GII.10 P domain residues that interacted with the 5B-18 Fab involved three sites on the P domain termed A, B, and C. The six GII.10 P domain residues that interacted with the 5B-18 Fab are indicated by light blue rectangles **(A)**. Left panel of **(B)**: a schematic of the VP1 deletion mutants. The construct 1 includes the N-terminal region and shell domain of VP1, and amino acids 4–223 from the N-terminal methionine of VP1. The P1-1 and P2 domain constructs without binding site A are construct 2 (amino acids 224–426), with binding site A is construct 4 (amino acids 224–439). Construct 3 has all binding sites A, B and C (amino acids 427–548). Construct 5 deletes binding site A from construct 3 (amino acids 440–548). Right panel of **(B)**: western blotting results with 5B-18. Samples indicated as VLP, NC (negative control), mutant construct 1 (#1), #2, #3, #4 and #5. The black arrow represents VLP band at 58 kDa, and the white arrows represent #3 and #5 products at 13 kDa.

IgG flexibility is not unknown. For example, a neutralizing antibody 9C12 binds to hexon, the major coat protein of adenovirus, at a ratio of 240 antibody molecules to one virus particle or one antibody per hexon trimer (Varghese et al., 2004). By dynamic light scattering and negative-stain EM, electron-dense material coats the virus, but it was not aggregated at neutralizing ratios. In images reconstructed from cryo-EM, the viral surface was covered by electron density from the 9C12 antibody. Two Fab arms bridge two peripentonal hexons. One has a normal Fab shape and fitted the models well (Harris et al., 1998). The other arm has a somewhat distorted structure. A low-density tail extends to a third hexon that forms a minor alternate binding site. The normal arm binds to a unique site in the asymmetric unit of the virus. It has no alternate binding sites because a penton, rather than a hexon, is positioned at the icosahedral fivefold axis. In addition, the angle between the long axes of the Fabs was $<115°$ that was found in the uncomplexed IgG1 (Harris et al., 1998). Thus, flexibility is important for the bivalent binding of 9C12.

ESTIMATING THE FLEXIBILITY IN THE STRUCTURE

The findings from the 9C12 study were informative for our 5B-18 paradox. 5B-18 could reach the bottom of the P domain if the Fab domain could bend and escape the P1 subdomain or star-like structure on the shell. 5B-18 IgG bound equally well with intact and partially broken GII.10 VLPs. To determine if 5B-18 binds to intact or broken particles, we took advantage of a characteristic of norovirus VLPs: they are less stable and appear to be broken at high pHs (Ausar et al., 2006). Therefore, we looked at 5B-18 binding at different pHs. At low and neutral pHs (5.3, 6.3, and 7.3), the GII.10 VLPs were mostly homogenous in size and unbroken, but at higher pHs (8.3 and 9.3), they were less homogenous and partially broken. 5B-18 IgG bound to GII.10 VLPs at different pH values with nearly identical efficacies, regardless of the fraction of damaged particles. At pH 5.3, 6.3, and 8.3, the titer was 512,000. At pH 9.3, it was 1,024,000, and at pH 7.3, it was 2,048,000 (optical density cutoff of 0.2; Hansman et al., 2006). We also determined size distribution of the VLPs by dynamic light scattering in each pH conditions. VLPs were shown single peak on diameter 38 to 50 nm (data not shown). These results suggest that 5B-18 appears detects nominally intact GII.10 VLPs.

We studied the 5B-18 binding mechanism by x-ray crystallography, molecular virology, and cryo-EM. We combined the results in *in silico* modeling that simulates molecular dynamics and is a reliable method for revealing fluctuations in protein structure. Each technique complemented the other by filling in for data that was lacking from the others. Interestingly, the 5B-18 study suggests that VLP and viral virion have structure flexibility and that IgG molecule have flexible arms. They co-work each other and bind. *In silico* modeling is clearly a powerful tool for enhancing our understanding of basic viral processes.

ACKNOWLEDGMENTS

We thank P. Kwong and his lab members for their guidance in this work and for critical discussions about structural analysis and K. Nagayama and K. Murata for assistance with the cryo-electron microscopy and for discussions. We also thank H. Sato for giving us this great opportunity to publish our studies.

REFERENCES

Ausar, S. F., Foubert, T. R., Hudson, M. H., Vedvick, T. S., and Middaugh, C. R. (2006). Conformational stability and disassembly of Norwalk virus-like particles. Effect of pH and temperature. *J. Biol. Chem.* 281, 19478–19488.

Bhella, D., Gatherer, D., Chaudhry, Y., Pink, R., and Goodfellow, I. G. (2008). Structural insights into calicivirus attachment and uncoating. *J. Virol.* 82, 8051–8058.

Bhella, D., and Goodfellow, I. G. (2011). The cryo-electron microscopy structure of feline calicivirus bound to junctional adhesion molecule A at 9-angstrom resolution reveals receptor-induced flexibility and two distinct conformational changes in the capsid protein VP1. *J. Virol.* 85, 11381–11390.

Guix, S., Asanaka, M., Katayama, K., Crawford, S. E., Neill, F. H., Atmar, R. L., et al. (2007). Norwalk virus RNA is infectious in mammalian cells. *J. Virol.* 81, 12238–12248.

Hansman, G. S., Biertumpfel, C., Georgiev, I., McLellan, J. S., Chen, L., Zhou, T., et al. (2011). Crystal structures of GII.10 and GII.12 norovirus protruding domains in complex with histo-blood group antigens reveal details for a potential site of vulnerability. *J. Virol.* 85, 6687–6701.

Hansman, G. S., Natori, K., Shirato-Horikoshi, H., Ogawa, S., Oka, T., Katayama, K., et al. (2006). Genetic and antigenic diversity among noroviruses. *J. Gen. Virol.* 87(pt 4), 909–919.

Hansman, G. S., Taylor, D. W., McLellan, J. S., Smith, T. J., Georgiev, I., Tame, J. R., et al. (2012). Structural basis for broad detection of genogroup II noroviruses by a monoclonal antibody that binds to a site occluded in the viral particle. *J. Virol.* 86, 3635–3646.

Harris, L. J., Skaletsky, E., and McPherson, A. (1998). Crystallographic structure of an intact IgG1 monoclonal antibody. *J. Mol. Biol.* 275, 861–872.

Jiang, X., Graham, D. Y., Wang, K. N., and Estes, M. K. (1990). Norwalk virus genome cloning and characterization. *Science* 250, 1580–1583.

Jiang, X., Wang, M., Graham, D. Y., and Estes, M. K. (1992). Expression, self-assembly, and antigenicity of the Norwalk virus capsid protein. *J. Virol.* 66, 6527–6532.

Lambden, P. R., Caul, E. O., Ashley, C. R., and Clarkel, N. (1993). Sequence and genome organization of a human small round-structured (Norwalk-like) virus. *Science* 259, 516–519.

Li, X., Zhou, R., Tian, X., Li, H., and Zhou, Z. (2010). Characterization of a cross-reactive monoclonal antibody against Norovirus genogroups I, II, III and V. *Virus Res.* 151, 142–147.

Lindesmith, L. C., Beltramello, M., Donaldson, E. F., Corti, D., Swanstrom, J., Debbink, K., et al. (2012) Immunogenetic mechanisms driving norovirus GII.4 antigenic variation. *PLoS Pathog.* 8, e1002705. doi: 10.1371/journal.ppat.1002705

Pettersen, E. F., Goddard, T. D., Huang, C. C., Couch, G. S., Greenblatt, D. M., Mengm, E. C., et al. (2004). UCSF Chimera – a visualization system for exploratory research and analysis. *J. Comput. Chem.* 25, 1605–1612.

Prasad, B. V., Hardy, M. E., Dokland, T., Bella, J., Rossmann, M. G., and Estes, M. K. (1999). X-ray crystallographic structure of the Norwalk virus capsid. *Science* 286, 287–290.

Prasad, B. V., Matson, D. O., and Smith, A. W. (1994). Three-dimensional structure of calicivirus. *J. Mol. Biol.* 240, 256–64.

Taube, S., Rubin, J. R., Katpally, U., Smith, T. J., Kendall, A., Stuckey, J. A., et al. (2010). High-resolution x-ray structure and functional analysis of the murine norovirus 1 capsid protein protruding domain. *J. Virol.* 84, 5695–705.

Varghese, R., Mikyas, Y., Stewart, P. L., and Ralston, R. (2004). Postentry neutralization of adenovirus type 5 by an antihexon antibody. *J. Virol.* 78, 12320–12332.

Wobus, C. E., Thackray, L. B., and Virgin, H. W. 4th. (2006). Murine norovirus: a model system to study norovirus biology and pathogenesis. *J. Virol.* 80, 5104–5112.

Yoda, T., Suzuki, Y., Terano, Y., Yamazaki, K., Sakon, N., Kuzuguchi, T., et al. (2003). Precise characterization of norovirus (Norwalk-like virus)-specific monoclonal antibodies with broad reactivity. *J. Clin. Microbiol.* 41, 2367–2371.

Zheng, D. P., Ando, T., Fankhauser, R. L., Beard, R. S., Glass, R. I., and Monroe, S. S. (2006). Norovirus classification and proposed strain nomenclature. *Virology* 346, 312–323.

Conflict of Interest Statement: The authors declare that the research was

conducted in the absence of any commercial or financial relationships that could be construed as a potential conflict of interest.

Received: 14 August 2012; paper pending published: 24 August 2012; accepted: 18 October 2012; published online: 06 November 2012.

Citation: Miki M and Katayama K (2012) In silico 3D structure analysis accelerates the solution of a real viral structure and antibodies docking mechanism. Front. Microbio. 3:387. doi: 10.3389/fmicb.2012.00387
This article was submitted to Frontiers in Virology, a specialty of Frontiers in Microbiology.

Microbiology and Immunology

Microbiol Immunol 2012; **56**: 760–770
doi:10.1111/j.1348-0421.2012.00499.x

ORIGINAL ARTICLE

Novel monoclonal antibodies broadly reactive to human recombinant sapovirus-like particles

Noritoshi Kitamoto[1], Tomoichiro Oka[2,3], Kazuhiko Katayama[2], Tian-Cheng Li[2], Naokazu Takeda[4], Yoji Kato[1], Tatsuya Miyoshi[5] and Tomoyuki Tanaka[5]

[1]School of Human Science and Environment, University of Hyogo, Hyogo 670-0092, [2]Department of Virology II, National Institute of Infectious Diseases, Tokyo 208-0011, [3]Food Animal Health Research Program, Ohio Agricultural Research and Development Center, Department of Veterinary Preventive Medicine, Ohio State University, Wooster, 44691, OH, USA, [4]Thailand-Japan Research Collaboration Center on Emerging and Re-emerging Infections, Nonthaburi 11000, Thailand, and [5]Sakai City Institute of Public Health, Osaka 590-0953, Japan.

ABSTRACT

Sapovirus (SaV), a member of the family *Caliciviridae*, is an important cause of acute epidemic gastroenteritis in humans. Human SaV is genetically and antigenically diverse and can be classified into four genogroups (GI, GII, GIV, and GV) and 16 genotypes (7 GI [GI.1–7], 7 GII, [GII.1–7], 1 GIV and 1 GV), based on capsid sequence similarities. Monoclonal antibodies (MAbs) are powerful tools for examining viruses and proteins. PAI myeloma cells were fused with spleen cells from mice immunized with a single type of recombinant human SaV virus-like particles (VLPs) (GI.1, GI.5, GI.6, GII.3, GIV, or GV). Sixty-five hybrid clones producing MAbs were obtained. Twenty-four MAbs were characterized by ELISA, according to their cross-reactivity to each VLP (GI.1, GI.5, GI.6, GII.2, GII.3, GII.4, GII.7, GIV, and GV). The MAbs were classified by this method into: (i) MAbs broadly cross-reactive to all GI, GII, GIV and GV strains; (ii) those reactive in a genogroup-specific; and (iii) those reactive in a genotype-specific manner. Further analysis of three broadly cross-reactive MAbs with a competitive ELISA demonstrated that at least two different common epitopes are located on the capsid protein of human SaVs in the four genogroups. The MAbs generated and characterized in this study will be useful tools for further study of the antigenic and structural topography of the human SaV virion and for developing new diagnostic assays for human SaV.

Key words cross-reactivity, monoclonal antibody, sapovirus.

Sapovirus, a member of the family *Caliciviridae*, causes gastroenteritis in humans and is a significant public health problem (1–5). SaV was originally identified by EM of fecal specimens obtained during a gastroenteritis outbreak (6, 7).

The SaV capsid is composed of 90 dimers of capsid protein (VP1) (8). SaV has a ~7.5 kb genome of single-stranded positive-sense RNA that is predicted to encode two or three ORFs. The functions of proteins encoded by ORF2 and ORF3 are unknown. However, ORF1 encodes nonstructural proteins and VP1 (9, 10). VP1 is likely produced by cleavage of the ORF1 polyprotein by viral protease or by translation from subgenomic RNA (3′-coterminal with the virus genome), or both (11, 12). A tripeptide, MEG, conserved among human SaV strains, is probably the putative VP1 start on the subgenomic RNA.

Correspondence
Noritoshi Kitamoto, School of Human Science and Environment, University of Hyogo, 1-1-12, Shinzaike-Honcho, Himeji-shi, Hyogo 670-0092, Japan. Tel: +81 792 92 9326; Fax: +81 792 92 9326; email: kitamoto@shse.u-hyogo.ac.jp

Received 4 July 2012; revised 2 August 2012; accepted 3 August 2012.

List of Abbreviations: CBB, Coomassie brilliant blue; DAB, diaminobenzidine; EM, electron microscopy; G, genogroup; HRPO, horseradish peroxidase; MAb, monoclonal antibody; NoV, norovirus; OD, optical density; OPD, ortho-phenylenediamine; ORF, open reading frame; P domain, protrusion domain; TPBS, Tween 20 phosphate-buffered saline; S domain, shell domain; SaV, sapovirus; *Sf9*, *Spodoptera frugiperda*; VLP, virus-like particles; VP1, capsid protein; WB, western blotting.

VP1 expressed from the putative subgenomic RNA or putative VP1-encoding construct in insect or mammalian cells self-assembles into virus-like particles that are morphologically similar to native SaV (12, 13–20). SaV VP1 has an apparent molecular mass of 60 kDa (11, 12, 21). Based on their complete VP1 sequences, SaVs are classified into at least five genogroups: GI, GII, GIII, GIV and GV. GI, GII, GIV and GV infect humans, and GIII infects porcine species (9). Human SaVs can be further separated into 16 genetic clusters (seven GI [GI.1–7], seven GII, [GII.1–7], one GIV and one GV) (22).

Because there is no cell-culture system or small-animal model for human SaV, SaV VLPs have been used as models of SaV virion for immunogenic, antigenic and structural studies. The capsid proteins of human SaVs have high antigenic diversity (16, 17, 20, 21, 23). However, little information is available about whether specific regions of the VP1 are important for antigenic specificity, and whether type-specific and/or cross-reactive epitopes are present in SaVs.

Monoclonal antibodies are powerful tools for the study of viruses and proteins. A panel of MAbs against SaV VLPs would be valuable for antigenic and structural analysis as well as useful for developing new diagnostic assays for human SaV. In this study, we established such a panel of MAbs broadly cross-reactive to all human SaV genogroups, GI, GII, GIV and GV, as well as MAbs specific to either genogroups or genotypes.

MATERIALS AND METHODS

Generation of recombinant baculoviruses

DNA fragments corresponding to the putative subgenomic RNA region of the genome (approximately 2.3 kb in length) of GI.6 Nichinan (GenBank accession number AB455803 [24]), GII.3 20082029 (AB630068 [22]), GII.3 D1711 (AB522391 [25]), GII.3 Kushiro5 (AB455793 [26]), GII.3 Nayoro4 (AB455794 [26]), GII.4 Kumamoto6 (AB429084 [1, 22]), GII.7 20072248 (AB630067 [22]), and GIV Yakumo8 (AB455795 [26]) were amplified by PCR with KOD-Plus-DNA polymerase (Toyobo) as previously described (27). A forward primer (5′-CAGATCTGCA GCGGCCGCATGGAGGN$_{8-10}$ [N indicates strain specific sequence]-3′) included a NotI site (underlined), and a common reverse primer (5′-GTCCCAGGAAAGGATCC TTTTTTTTTTTTTTTTTTTTTTTTTTTTT-3′) included a BamHI site (underlined). The amplified fragments were cloned into NotI- and BamHI-digested baculovirus transfer vector pVL1392 (Orbigen, San Diego, CA, USA) with an In-Fusion Advantage PCR Cloning Kit (Takara, Shiga, Japan), according to the manufacturer's protocol. *Escherichia coli* HST08 premium competent cells (Takara) were used to transform and propagate the transfer plasmid. Sequencing analysis confirmed the consensus sequence of each strain. An insect cell line derived from *Sf9* (Riken Cell Bank, Tsukuba, Japan) was co-transfected with a linearized wild-type *Autographa californica* nuclear polyhedrosis virus DNA (Baculo-Gold, BD Bioscience, Franklin Lakes, NJ, USA) and the transfer vectors carrying the human SaV putative subgenomic RNA region by the lipofectin-mediated method as specified by the manufacturer (Gibco BRL, Gaithersburg, MD, USA).

Expression and purification of human sapovirus virus-like particles

For larger scale expression of the SaV capsid proteins, BTl-Tn-5B1–4 (Tn5), an insect cell line derived from *Trichoplusia ni* (Invitrogen, San Diego, CA, USA), was infected with recombinant baculoviruses at a multiplicity of infection of 10 and incubated for 7 days at 26°C, as previously described (28). Eight novel VLPs derived from GI.6 Nichinan, GII.3 20082029, GII.3 D1711, GII.3 Kushiro5, GII.3 Nayoro4, GII.4 Kumamoto6, GII.7 20072248 and GIV Yakumo8 were purified as follows. Intact cells, cell debris, and progeny baculoviruses were removed by centrifugation at 10,000 *g* for 60 min. The supernatant was then centrifuged at 174,899 *g* for 3 hr in a Beckman SW32-Ti rotor rotor (Beckman Coulter, Fullerton, CA, USA). The resulting pellet was resuspended in EX-CELL 405 Serum Free medium (SAFC Biosciences, Lenexa, KS, USA) at 4°C overnight and the debris removed by centrifugation at 10,000 *g* for 30 min at 4°C. The supernatant was then centrifuged at 154,000 *g* for 2 hr in a Beckman TLA55. The resulting pellet was resuspended in EX-CELL 405 Serum Free medium (SAFC Biosciences) at 4°C overnight, and the debris removed by centrifugation at 10,000 *g* for 5 min at 4°C. After mixing with 2.1 g of CsCl in MilliQ water, the sample was centrifuged at 148,862 *g* for 24 hr at 10°C in a Beckman SW55-Ti rotor. After fractionation (20 × 250 μL each), each aliquot was diluted with EX-CELL 405 medium, and centrifuged at 154,000 *g* for 2 hr at 4°C in a Beckman Coulter TLA55 rotor. The resulting pellet was resuspended in EX-CELL 405 medium. Seven VLPs derived from GI.1 Mc114 (AY237422 [27]), GI.5 Yokote1 (AB253740 [17]), GII.2 Mc10 (AY237420 [10]), GII.3 C12 (AY603425 [10]), GII.3 Syd53 (DQ104360 [29]), GIV Syd3 (DQ104357 [29]) and GV NK24 (AY646856 [30]) were expressed and purified as previously described (14, 16, 17, 20).

Preparation of monoclonal antibodies

The PAI myeloma cell line (kindly provided by M. Kotani, Tokyo Metropolitan Institute of Medical Science,